CORRELATION BETWEEN BENDING TEST AND BARCELONA TESTS TO DETERMINE FRC PROPERTIES

SERGIO CARMONA[1]

Departamento de Obras Civiles, Universidad Técnica Federico Santa María

Valparaíso, Chile

CLIMENT MOLINS

and

ANTONIO AGUADO

Departamento de Ingeniería Civil y Ambiental,

Universitat Politècnica de Catalunya,

Barcelona, España

ABSTRACT

The use of fiber reinforced concretes (FRC) as a substitute for reinforcement meshes, particularly in the construction of tunnels, frequently faces quality control problems because the specifications and acceptability criteria are based on parameters obtained from the flexion test of standard EN – 14651, which is very difficult to perform at works. Considering the advantages presented by the Barcelona test, in this paper, equivalences are established between both tests, which allow estimating the FRC toughness and residual strengths. The predictions of these properties obtained using the Barcelona tests results present a maximum difference of less than 20%.

KEYWORDS: Barcelona test; residual strength; toughness; fiber reinforced concrete.

[1]Corresponding author: sergio.carmona@usm.cl, Casilla 110 – V Valparaíso, Chile. Tel. +56322654382 Fax +56322654115

1. INTRODUCTION

Toughness and residual strength are the main properties used to characterize the post-crack behavior of fiber-reinforced concrete and they are used in the constitutive equations for structural design (CEB, 2010; ACI 2014) and to classify and specify Fiber Reinforced Shotcrete (EFNARC, 1996; EN 14487 – 1, 2008). Toughness is a measure of the energy absorption capacity of a specimen, in terms of the area under the load – deflection curve and its magnitude depends directly on the geometry and test specimen and on the load configuration (ACI, 2017). Considering that after reaching the maximum load, the bulk concrete undergoes a softening, the residual strengths can be defined as the capacity of reinforced concrete to withstand load in the post – cracking stage.

Although the uniaxial or direct tensile test is considered the most appropriate method to determine the fracture properties of brittle materials, such a test is difficult to perform and its results exhibit great scatter due to the experimental difficulty of obtaining uniform tension distributions throughout the crack. This is due to the heterogeneity of the material, specimen imperfections and to eccentricities during the loading process. Moreover, there are further inconveniences, such as the fastening of the sample and difficulty in ensuring test stability when the material's cracking load is reached.

However, the Technical Committee of RILEM TC 162 (2002) has proposed a uniaxial traction test on notched samples. A study performed by Barragán *et al*. (2003) showed that this method is representative of the material response. Nonetheless, the post-cracking tensions and the toughness parameters obtained from this test exhibits coefficients of variation (CoV) of approximately 30%. This wide scatter of measured parameters difficult to apply this test for systematic FRC control.

Due to these experimental difficulties, FRC properties are determined and controlled at works by means of beams subjected to three points bending test (3PB) or third-point loading test (4PB). Such tests are characterized by results with high dispersions. In

addition, this type of test requires relatively heavy samples and complex experimental procedures, and their results show significant dispersions (Chao *et al*., 2012). This is due to their small fracture surface, usually with only one crack, and the properties depend directly on the specific number of fibers which cross the crack section, making them unsuitable for the control of FRC in works (Carmona *et al*., 2012). Furthermore, these results are also affected by the size of the specimen (Cavalaro *et al*., 2015).

With the aim of providing an adequate test for systematic FRC control at works, Molins *et al*. (2009) developed an indirect traction test based on the double – punch test, known as the "Barcelona (BCN)" test, which has been standardized as UNE 83 515 in Spain by AENOR (2010).

Due to its simplicity and greater knowledge of the response of the FRC subjected to the BCN test, supported by a large number of researches both at the experimental level (Carmona *et al*., 2013; Aire *et al*., 2015) and numerical (Pros *et al*., 2011; 2012; Pujadas *et al*., 2013), the BCN test is progressively being used to evaluate the post-cracking behavior of FRC (Chao *et al*., 2012; Kim *et al*., 2015; Carmona *et al*., 2016). It has also been used as a control test for fiber-reinforced shotcrete in several large projects, such as the Lima Metro (Geocontrol, 2015), the *Chuquicamata Subterránea* project of the Codelco – Chile mining company (Carmona, 2017), and linings for 22.5 km tunnel of Follo Line in Norway.

Considering that currently the equations and design criteria given by the Model Code MC – 2010 of CEB – FIP (CEB, 2010) are based on parameters defined in terms of the load – $CMOD$ (crack mouth opening displacement) response, obtained through flexion tests, which is suitable for the characterization of FRC, but difficult to implement for the systematic quality control in works, the main goal of this research is establishing a correlation between the FRC properties determined by means of bending test following European standard EN – 14651 and the BCN test. For this aim, the results obtained in

different experimental campaigns developed by the authors at the Universidad Técnica Federico Santa María of Valparaíso (UTFSM), Chile and at Universitat Politècnica de Catalunya (UPC), Barcelona, Spain, were used.

2. RESEARCH IMPORTANCE

The BCN test has proved to be an experimental procedure with an enormous potential to be used for the systematic quality control of FRC at works, due to its simplicity, stability and low scatter of its results. However, structural design codes and construction recommendations are based on properties determined using bending tests, which are complex to execute and their results exhibit high dispersions. Consequently, to implement the BCN test for the quality control at works requires to correlate their results with the properties obtained by means of the bending test. To obtain comparable values of toughness and residual strengths of FRC, an equivalence criterion between the flexural test and the double punching test based on crack opening is developed.

3. THREE-POINT BENDING FLEXURAL TESTS (3PB)

According to standard EN – 14651 (2005), the characterization of FRC properties is performed by testing a prismatic element of dimensions 600 mm × 150 mm × 150 mm under flexion with a central notch of 25 mm depth and loaded at the midspan (3PB). The test must be performed in a closed – loop control of the $CMOD$ at a rate of 0.05 mm/min and with a sufficiently high rigidity to avoid instabilities during the transition between the pre- and post-cracking regimes. During the test, the load and $CMOD$ is continuously recorded.

Using the *P – CMOD* response obtained during the test, standard EN 14651 defines the residual strengths $F_{R,j}$ as

$$\boldsymbol{F_{R,j} = \frac{3\,P_i\,l}{2\,b\,h_{sp}^2}} \quad (1)$$

where l = 500 mm, b = 150 mm, and h_{sp} = 125 mm correspond to the span, and the width and height of the specimen, respectively; P_i, with i = 1, 2, 3, 4, are the loads corresponding to the crack openings $CMOD_1$ = 0.5 mm, $CMOD_2$ = 1.5 mm, $CMOD_3$ = 2.5 mm, and$CMOD_4$ = 3.5 mm, respectively.

4. BARCELONA TEST

As Barcelona or BCN test is known a double-punch test proposed by Molins *et al*. (2009) to determine fiber reinforced concretes properties (ACI, 2016). This test consists of subjecting a cylindrical specimen of dimensions $d = h$ = 150 mm, i.e., h/d = 1, to compressive stress by means of two steel wedges of diameter $a = d/4$, as seen in Figure 1. This test is performed in a conventional testing system under stroke displacement control at a rate of 0.5 ± 0.05 mm/min.

The applied load, P, and the circumferential deformation ($TCOD$), which is measured at half the specimen height, must be recorded continuously during the test, obtaining the $P - TCOD$ relation.

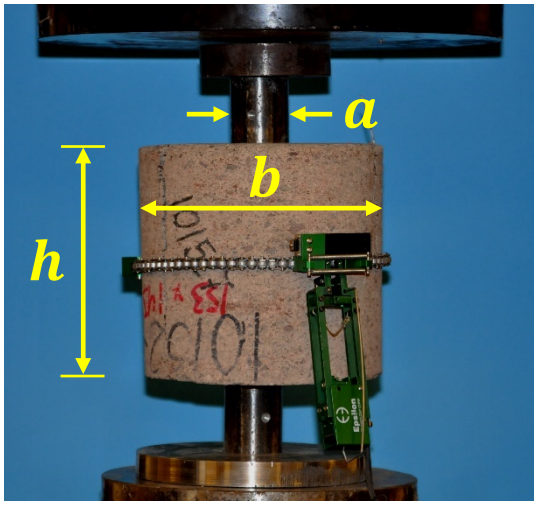

Figure 1. BCN test setup and test parameters.

During the test, the applied load produces a conical volume under triaxial compression stress just beneath the punches, which tend to increase the cylinder diameter and to produce tensile stresses perpendicular to the radial planes of specimen. Due to this tensile stress with cylindrical symmetry, when the stress exceeds the tensile strength of concrete, cracks perpendicular to the tension field propagate through the specimen. This allows compression cones to penetrate the cylinder increasing the specimen radius and producing two or more cracks, as can be seen in Figure 2. Then, the final state of the specimen present two aligned cracks or three cracks arranged approximately at 120° or, sometimes, four perpendicular cracks (Carmona *et al*., 2012).

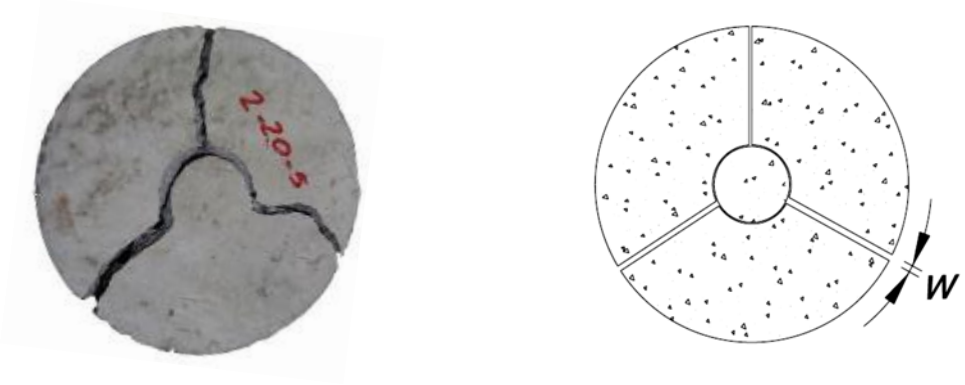

Figure 2. Average crack in the Barcelona test (photography and idealization).

When the cracks open due to tensile state on concrete, the circumferential deformation corresponds to the total crack opening displacement ($TCOD$) and the energy dissipated by the FRC during the fracture process can be calculated as:

$$E_{BCN}(TCOD) = \int_0^{TCOD} P(TCOD)d(TCOD) \quad (2)$$

where $E_{BCN}(TCOD)$ is the energy dissipated up to a given $TCOD$. At the same time, the tensile residual strength of the FRC, $f_{ct,Rx}$, which corresponds to a given circumferential deformation R_x, can be obtained with the following equation:

$$\boldsymbol{f_{ct,Rx} = \frac{4\,P_{R,x}}{9\,\pi aH}} \quad (3)$$

where a and H are the dimensions defined in Figure 1, and $P_{R,x}$ is the load at the circumferential deformation R_x (AENOR, 2010).

The BCN test presents a series of advantages over the flexural tests, among which the following stand out: (1) the use of relatively small cylindrical specimen, which can be molded, can be cut from standardized cylinders of dimensions d = 150 mm × h = 300 mm, or can be cores drilled from an existing structure; (2) a conventional testing frame is required for the compression test; and (3) a large fracture surface which allows quantifying the FRC properties through various fracture planes, The latter reduces the scatter of results (Carmona *et al*., 2012).

5. EQUIVALENCE BETWEEN THE 3PB AND BCN TESTS

To obtain comparable values between the 3PB and BCN tests, equivalence has been established for concrete crack opening. For this purpose, it has been assumed that, in advanced states of crack opening, the crack faces are completely separated and the beam is only joined at the top hinge of the fracture plane, as shown in Figure 3. Although this hypothesis is not completely true, particularly for low levels of deformation, it has been observed experimentally that the difference is not significant for large crack openings.

Considering that the flexion test records the $CMOD$ measured under the notch, the real crack opening ($2w$) is slightly smaller because it opens at the notch tip. According to the previous hypothesis, it can be assumed that at half the height of the fracture plane, i.e., at $h_{sp}/2$, one can determine the mean crack opening (w), as also shown in Figure 3b.

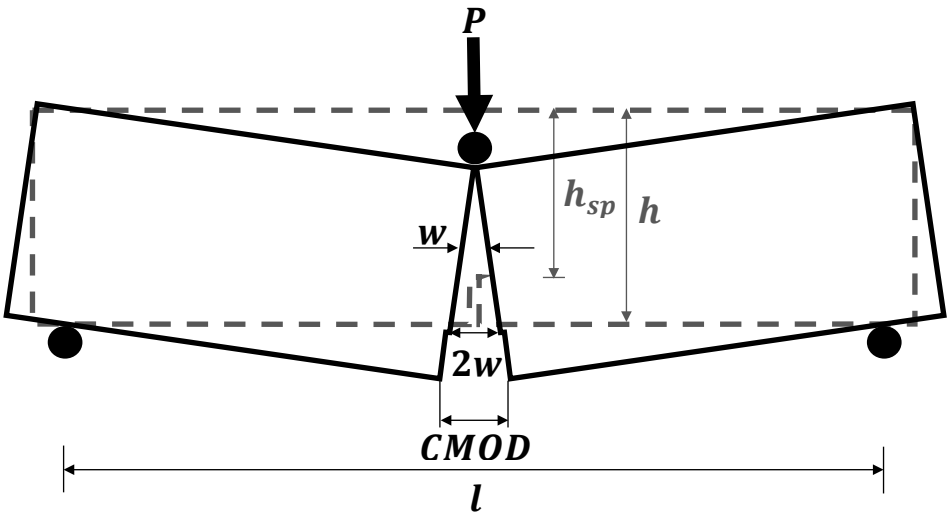

Figure 3. Simplified 3PB test schemes of beam failure and crack opening.

Then, the relation in expression (4) can be established.

$$w = \frac{h_{sp}}{2h} CMOD \tag{4}$$

In the BCN test, the failure of the specimen produces radial fracture planes and the value recorded during the test is the circumferential dilation or the diameter increase ($\Delta\phi$). When the specimen is fractured, this measurement is equivalent to the sum of the opening of all radial cracks or Total Circumferential Opening Displacement ($TCOD$).

Considering that usually appear three radial cracks separated 120°, as shown in Figure 2b, the mean crack opening (w) can be obtained as:

$$w = \frac{\Delta\phi}{3} = \frac{TCOD}{3} \tag{5}$$

Equating expressions (4) and (5), and considering that h = 150 mm, and h_{sp} = 125 mm yields a direct geometric relation between the $TCOD$ and the $CMOD$ (equation 6).

$$TCOD = 1.25\, CMOD \tag{6}$$

This equivalence between $CMOD$ and $TCOD$ allows relating comparable values between the FRC flexural toughness and the energy dissipated in the BCN test, and between the residual strengths of the material at cracked state. The equivalences presented in Table 1

were obtained using expression (6) and were used in this research to obtain comparable values between both tests.

Table 1. Equivalence between $TCOD$ and $CMOD$, and mean crack opening (w).

$CMOD$ (mm)	0.5	1.0	1.5	2.0	2.5	3.0	3.5
$TCOD$ (mm)	0.625	1.250	1.875	2.500	3.125	3.750	4.375
w (mm)	0.208	0.417	0.625	0.833	1.042	1.250	1.458

6. EXPERIMENTAL DETAILS

To establish correlations between the properties of different steel fiber reinforced concretes obtained with the 3PB and BCN tests, the results of four experimental campaigns carried out both in Barcelona and Valparaiso are used, which are described next.

6.1. Materials Studied

With the aim of obtaining general correlations applicable to different types of concrete, this research uses the results of several experimental programs led by the authors at both Universitat Politècnica de Catalunya (UPC) in Barcelona, Spain, and Universidad Federico Santa Maria (UTFSM) in Valparaiso, Chile. These experimental programs were reported in Molins *et al*. (2008), Monsó (2011), Aire *et al*. (2015) and Carmona (2016). According to the latter, seven different types of concrete were included in this research: two conventional concretes (C) with compressive strength of 30 MPa and 50 MPa and reinforced with 30 kg/m^3 and 50 kg/m^3 of fibers respectively; two self compacting concretes with normal and high compressive strength, designated as SCC – N and SCC-H respectively, both reinforced with two fiber amounts 20 kg/m^3 and 40 kg/m^3; a third self compacting concrete of normal strength (designated as M series) reinforced with 30 kg/m^3 of four different type of fibers with different length (l_f) and diameter (d_f), and almost identical aspect ratio ($\lambda_f = l_f/d_f$). Finally, a sprayed concrete designed to be used

as lining in mining tunnels, designated as SH and reinforced with 25 and 40 kg/m^3 of fibers.

The mixes proportions of the different concretes are presented in Table 2 and the geometric characteristics and mechanical properties of the different fibers are summarized in Table 3.

Table 2. Dosage of the concretes (kg/m^3).

Concrete		Cement	Water	Filler 500 μm	Sand 0/5 mm	Gravel		Admixture	
Type	Ref.					5/12 mm	12/20 mm	Type	dose
C	C	275	150	-	1062	106	773	Water reducer	0.83
								Plasticizer	1.93
SCC – N	A	334	167	100	939	447	328	Water reducer	6.35
SCC – H	B	436	197	132	803	804	-	Water reducer	12.3
SCC – N	M	350	178	300	510	400	520	Water reducer	12
SH	SH	420	215	-	1535	120	-	Plasticizer	2.10
								Water reducer	2.10
								Rheology control	2.94

Table 3. Properties of the fibers (l_f, d_f, f_{st} are manufacturer data).

Concrete		Fiber	l_f (mm)	d_f (mm)	λ_f l_f/d_f	f_{st} (MPa)	N° Fibers/kg
Type	Reference						
C	C	Dramix RL-45/50-BN©	50	1.05	47.6	1115	2800
SCC – N	A	Dramix RC-80/60 BP©	60	0.71	84.5	2300	5000
SCC – H	B						
SCC – N	M1	Dramix RC-65/35-BN©	35	0.55	63.6	1345	14704
	M2	Dramix RC-65/40-CN©	40	0.62	64.5	1440	10000
	M3	Wirand FF3-50©	50	0.75	66.7	1230	5405
	M4	Dramix RC-65/60-BN©	60	0.90	71.2	1160	3226

SH	SH	Dramix 3D 65/35 BG	35	0.55	63.6	1345	14531

All the studied concretes were prepared in vertical axis mixers and the cylinder specimens were molded of dimensions $h = d = 150$ mm, i.e., $h/d = 1$, for the BCN test and standardized beams of dimensions $b = 150$ mm × $h = 150$ mm × $l = 600$ mm for the flexural tests. To determine the compressive strength of each concrete, three $d \times h = 150$ mm × 300 mm standardized cylinders were also molded. The details regarding the number of specimens of each type are presented in Table 4. All the specimens were kept in a fog room until testing. Table 4 also shows the strength and the testing age of each type of concrete with the fiber content in kg/m^3 and the volumetric substitution (V_f) in percentage.

Table 4. Number of significant results and features of the tested concretes.

Concrete		Type of specimen		Testing age (days)	f_c (MPa)	Fibers content (kg/m^3)	V_f (%)
Type	Reference	Cylinder BCN $b \times h$ (mm)	Beam $b \times h \times l$ (mm)				
		150×150	150×150×600				
C	C30	10	15	28	45	30	0.385
	C50	10	12		44	50	0.641
SCC–N	A40	10	5		46	40	0.513
	A60	10	5		50	60	0.769
SCC–H	B40	6	6		76	40	0.513
	B60	6	6		79	60	0.769
SCC–N	M1	6	6	55	55	30	0.385
	M2	6	5	49	58		
	M3	6	6	57	58		
	M4	6	6	55	55		
SH	SH25	13	10	28	41	25	0.321
	SH40	13	10		45	40	0.513

6.2. Flexion tests

In the tests performed at the UPC in Barcelona, the 3PB ones were performed in an Instron servohydraulic system of a static capacity of 1.0 MN with a feedback loop control under crack opening control at a rate of 0.05 mm/min until reaching an opening of 0.1 mm. Then, the speed was increased to 0.2 mm/min until the end of the test. Before to the flexion tests, a 25-mm deep notch was made in the beams at their span center. The test setup was conducted according to standard EN – 14651. On the other hand, the bending tests performed at the UTFSM in Valparaiso were performed on a Controls system with a capacity of 100 kN under crack opening displacement control at the rate given by the standard, which was measured with a clip-gauge extensometer with a total range of 5.0 mm.

During the tests, the load and $CMOD$ were recorded, obtaining the typical curves shown in Figure 4, for each of the tested concretes. In the $P - CMOD$ diagrams, different behaviors were observed in the post-cracking regime, which vary from softening to hardening, depending on the aspect ratio, λ_f, and fiber content. Moreover, an effect of concrete workability can be seen in the curves obtained with each series, differentiating between conventional concretes (C) with 8 cm slump, self-compacting concretes (SCC), and shotcrete (SH), where the increase of concrete fluidity contributes to orient the fibers perpendicular to direction of casting, which was also observed by Laranjeira *et al*. (2012) and Blanco *et al*. (2015).

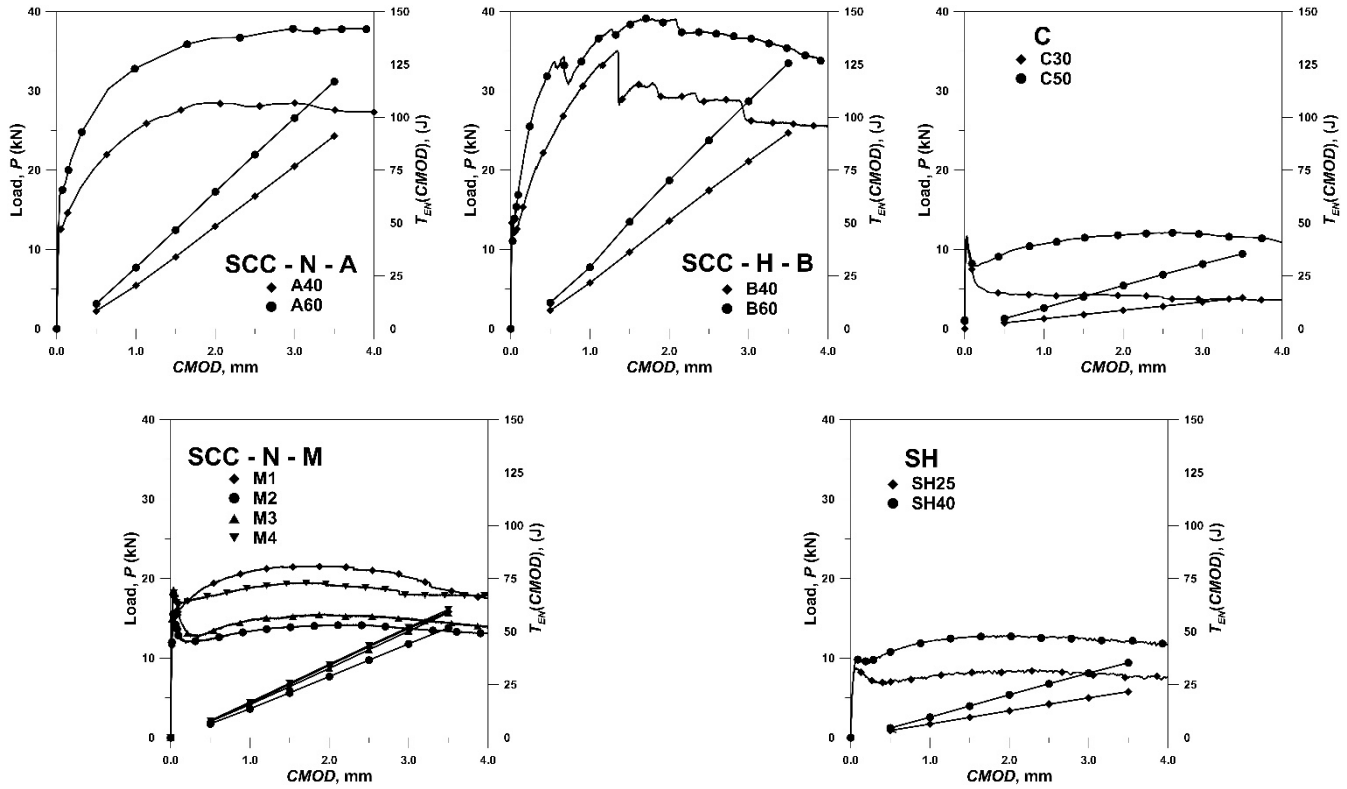

Figure 4. Typical $P-CMOD$ curves obtained in the 3PB tests and average bending toughness, $T_{EN}(CMOD)$ for each FRC.

Using the P – $CMOD$ responses obtained from each test, the flexural toughness $T_{EN}(CMOD)$ of each FRC was calculated with the expression:

$$T_{EN}(CMOD) = \int_0^{CMOD} P(CMOD)d(CMOD) \quad (7)$$

where $P(CMOD)$ is the load corresponding at a given $CMOD$. The average values of $T_{EN}(CMOD)$ obtained with each tested FRC are plotted in Figure 4 and presented in Table 5 along with their respective variation coefficients in brackets. The values of the variation coefficients in Table 5 show high variability of the flexural test results, particularly for the conventional concretes, where there is presumably a lower degree of orientation of the fibers. This confirms the trends observed in previous researches (Carmona *et al.*, 2011) and demonstrates one of the weaknesses of the three points bending test.

Table 5. Average values of flexural toughness, $T_{EN}(CMOD)$, in Joules (J).

$CMOD$ (mm)			0.5	1.0	1.5	2.0	2.5	3.0	3.5
Concrete	C	C30	2.8 (19.4)	4.8 (27.3)	6.9 (31.1)	9.0 (33.3)	11.1 (35.1)	13.1 (36.5)	15.2 (38.4)
		C50	4.8 (20.2)	9.8 (25.0)	15.1 (27.7)	20.4 (29.7)	25.7 (31.1)	30.6 (31.1)	35.4 (31.1)
	SCC – N	A40	8.9 (9.2)	20.9 (8.7)	34.6 (8.4)	49.0 (7.8)	63.2 (7.5)	77.4 (7.5)	91.8 (7.7)
		A60	11.9 (11.0)	29.0 (11.0)	46.8 (11.5)	64.9 (11.2)	82.1 (11.4)	98.6 (12.3)	115.4 (12.3)
		M1	7.7 (11.6)	16.2 (15.0)	25.1 (16.5)	34.0 (17.5)	42.9 (18.2)	51.4 (18.7)	59.4 (19.0)
		M2	6.5 (15.8)	13.6 (19.2)	21.1 (20.4)	28.8 (20.8)	36.5 (21.0)	44.2 (21.2)	51.7 (21.4)
		M3	7.6 (6.2)	15.6 (7.2)	24.0 (7.8)	32.7 (8.5)	41.5 (9.0)	50.2 (9.4)	58.8 (9.7)
		M4	8.0 (6.1)	16.7 (5.4)	25.6 (5.7)	34.6 (6.0)	43.4 (6.2)	52.0 (6.4)	60.4 (6.7)
	SCC – H	B40	8.6 (25.7)	21.7 (24.2)	36.3 (21.2)	51.1 (19.1)	65.4 (17.8)	79.2 (17.1)	92.6 (16.4)
		B60	12.3 (21.1)	29.1 (32.7)	50.6 (12.8)	70.2 (11.5)	89.1 (11.4)	107.6 (11.5)	125.6 (11.8)
	SH	SH25	3.4 (17.3)	6.4 (22.6)	9.5 (25.4)	12.7 (26.9)	15.8 (27.8)	18.8 (28.4)	21.7 (28.8)
		SH40	4.5 (15.8)	9.6 (21.0)	14.9 (23.4)	20.2 (24.5)	25.4 (25.2)	30.4 (25.7)	35.3 (26.1)

On the other hand, using the equation (1) given in standard EN – 14651, the residual strength $F_{R,j}$ was calculated, yielding the average values shown in Table 6, where the variation coefficients obtained with each tested FRC series are included in brackets.

Table 6. Average values of residual strength, $F_{R,j}$, obtained by means of 3PB tests, in (MPa)

CMOD (mm)			0.5	1.0	1.5	2.0	2.5	3.0	3.5
Concrete	C	C30	1.26 (35.4)	1.30 (39.7)	1.32 (39.6)	1.30 (43.5)	1.29 (45.1)	1.26 (45.4)	1.20 (48.1)
		C50	3.05 (27.8)	3.29 (30.9)	3.35 (31.9)	3.35 (36.5)	3.31 (36.5)	3.09 (33.0)	3.00 (32.7)
	SCC – N	A40	6.87 (9,9)	8.27 (9.0)	9.01 (7.9)	9.39 (6.3)	9.01 (10.5)	9.21 (8.8)	9.17 (10.1)

		A60	9.98 (12.2)	11.77 (11.1)	11.41 (13.4)	11.51 (9.9)	11.20 (12.0)	11.07 (9.6)	10.99 (9.1)
		M1	5.26 (16.6)	5.61 (19.0)	5.74 (19.9)	5.71 (20.4)	5.57 (21.1.)	5.30 (21.3)	4.95 (20.8)
		M2	4.32 (21.1)	4.71 (23.2)	4.89 (22.1)	4.95 (21.6)	4.95 (22.0)	4.85 (22.3)	4.75 (22.5)
		M3	4.83 (8.1)	5.31 (8.8)	5.47 (10.2)	5.60 (11.0)	5.64 (11.3)	5.57 (11.7)	5.46 (11.6)
		M4	5.40 (5.0)	5.66 (6.2)	5.74 (7.1)	5.71 (7.7)	5.57 (7.3)	5.43 (7.6)	5.29 (9.9)
	SCC – H	B40	7.43 (26.4)	8.85 (18.9)	9.47 (15.8)	9.47 (13.8)	8.87 (13.9)	8.68 (14.2)	8.48 (13.5)
		B60	10.91 (14.2)	11.59 (16.7)	12.66 (10.0)	12.41 (9.2)	11.97 (13.0)	11.64 (14.6)	11.34 (15.1)
	SH	SH25	1.98 (22.4)	2.09 (25.4)	2.13 (25.7)	2.12 (26.0)	2.06 (26.1)	2.00 (24.6)	1.93 (24.7)
		SH40	3.06 (24.3)	3.35 (27.3)	3.39 (29.0)	3.36 (28.0)	3.27 (28.0)	3.16 (29.0)	3.06 (29.0)

6.3. BCN Tests

At the UPC in Barcelona, the BCN tests were performed using the configuration given in standard UNE 83 515 (AENOR, 2010) with an Ibertest hydraulic system (model MEH 3000W) with a capacity of 3.0 MN under displacement control by an actuator at a rate of 0.5 ± 0.05 mm/min. The *TCOD* was measured with a MTS circumferential extensometer (model 632.12F-20) placed at half the specimen height. The load, P, and the $TCOD$ were recorded continuously during the tests by means of a Hewlett Packard 34970a data acquisition system.

On the other hand, at UTFSM in Valparaiso, the tests were performed in a Toni Technik hydraulic system of 3.0 MN of capacity under displacement control, following the specifications and configuration given in standard UNE 83 515. The circumferential deformation was recorded with an Epsilon extensometer (model 3544) with a total range of 12 mm, and the data were recorded by a Hewlett Packard model 7500 – XVI system.

Figure 5 shows the typical $P - TCOD$ curves obtained with each of the tested concretes. In all of them, it can be observed that there is no circumferential deformation until the

peak load is reached and, in the post-cracking regime, all the FRC specimens exhibit a softening behavior governed by the aspect ratio and the fiber content of each concrete.

The energy dissipated by FRCs during the BCN test was calculated using expression (2) and the results are presented in Table 7 and plotted in Figure 5. According to expression (6), the *TCOD* values in Table 7 are equivalent to the *CMOD* values used in Table 5 for the flexural toughness. In Table 7, the variation coefficient of each concrete's results is indicated in brackets. These variation coefficients are considerably lower than those obtained from the bending tests included in Table 5, which verifies one of the advantages of the BCN test.

On the other hand, Table 8 includes the residual strength values calculated using expression (3) given by standard UNE 83515 for the *TCOD* values equivalent to the *CMOD* values given in Table 6.

Table 7. Average values of $E_{BCN}(TCOD)$, in Joules (J).

TCOD (mm)			0.625	1.250	1.875	2.500	3.125	3.750	4.375
Concrete	C	C30	58.1 (10.0)	104.0 (9.6)	141.2 (9.6)	172.9 (9.8)	200.9 (10.2)	226.0 (10.6)	248.2 (10.8)
		C50	64.1 (7.3)	115.4 (7.9)	157.7 (8.8)	193.8 (9.5)	225.3 (10.3)	253.1 (11.0)	277.7 (11.6)
	SCC – N	A40	74.4 (8.9)	137.4 (6.6)	196.0 (6.4)	249.4 (6.4)	299.6 (6.5)	346.7 (6.7)	391.2 (6.8)
		A60	75.1 (5.0)	137.8 (5.9)	195.0 (7.4)	247.8 (8.3)	297.5 (8.7)	344.7 (8.6)	389.3 (8.3)
		M1	75.0 (4.1)	135.2 (5.2)	183.1 (4.5)	223.1 (4.6)	257.5 (4.8)	287.5 (5.3)	314.0 (6.0)
		M2	61.7 (10.9)	107.8 (6.2)	140.9 (7.0)	169.9 (7.9)	196.3 (8.9)	220.5 (9.9)	242.7 (10.8)
		M3	62.8 (22.6)	123.1 (5.1)	159.8 (5.4)	191.2 (5.5)	219.6 (5.8)	245.8 (6.1)	270.2 (6.2)
		M4	74.4 (8.5)	135.3 (10.3)	183.6 (11.6)	223.5 (12.1)	258.2 (12.5)	289.2 (12.8)	317.5 (13.2)
	SCC – H	B40	82.3 (9.6)	157.3 (9.4)	225.3 (10.4)	285.7 (10.1)	339.8 (9.8)	389.0 (9.9)	433.6 (9.7)
		B60	81.1 (6.8)	161.9 (6.4)	236.0 (7.0)	301.5 (7.7)	360.2 (8.0)	412.8 (8.3)	461.3 (8.6)

	SH	SH25	41.9 (16.7)	80.1 (14.5)	109.6 (14.8)	128.2 (16.6)	145.9 (17.8)	162.1 (18.9)	176.9 (19.8)
		SH40	47.1 (20.8)	83.9 (19.2)	112.3 (18.9)	136.9 (18.6)	159.0 (18.4)	179.5 (18.4)	198.3 (18.4)

1

2 Table 8. Average values of $f_{ct,Rx}(TCOD)$, in (MPa).

TCOD (mm)			0.625	1.250	1.875	2.500	3.125	3.750	4.375
Concrete	C	C30	2.04 (11.0)	1.62 (12.2)	1.37 (12.9)	1.19 (14.0)	1.06 (15.4)	0.95 (15.8)	0.85 (15.1)
		C50	2.26 (10.5)	1.84 (11.3)	1.57 (12.8)	1.35 (14.8)	1.18 (15.8)	1.05 (18.0)	0.95 (18.5)
	SCC – N	A40	2.62 (6.8)	2.41 (7.7)	2.24 (7.3)	2.08 (7.4)	1.95 (7.9)	1.84 (9.5)	1.74 (11.1)
		A60	2.63 (9.6)	2.41 (11.6)	2.19 (11.4)	2.05 (11.1)	1.92 (9.6)	1.83 (7.9)	1.73 (6.2)
		M1	2.67 (7.4)	2.22 (4.3)	1.81 (6.3)	1.52 (11.2)	1.29 (14.2)	1.11 (18.1)	0.97 (20.5)
		M2	2.09 (7.6)	1.43 (11.9)	1.22 (12.2)	1.10 (15.0)	1.00 (18.7)	0.92 (20.6)	0.84 19.6)
		M3	2.53 (10.3)	1.64 (11.2)	1.32 (9.7)	1.18 (9.6)	1.08 (9.5)	1.00 (9.1)	0.94 (9.5)
		M4	2.72 (10.5)	2.12 (14.7)	1.73 (15.5)	1.46 (14.8)	1.30 (16.2)	1.17 (18.9)	1.08 (18.9)
	SCC – H	B40	3.11 (10.9)	2.91 (13.3)	2.57 (11.7)	2.29 (9.8)	2.08 (11.8)	1.89 (12.7)	1.70 (13.9)
		B60	3.87 (8.0)	3.36 (9.8)	3.26 (12.2)	2.88 (12.1)	2.58 (12.1)	2.34 (13.3)	2.14 (13.4)
	SH	SH25	1.64 (14.4)	1.19 (20.0)	0.86 (25.6)	0.73 (27.7)	0.67 (29.5)	0.61 (31.2)	0.59 (31.5)
		SH40	1.64 (7.9)	1.24 (16.7)	1.04 (16.5)	0.92 (17.8)	0.84 (19.4)	0.78 (21.1)	0.72 (21.6)

3

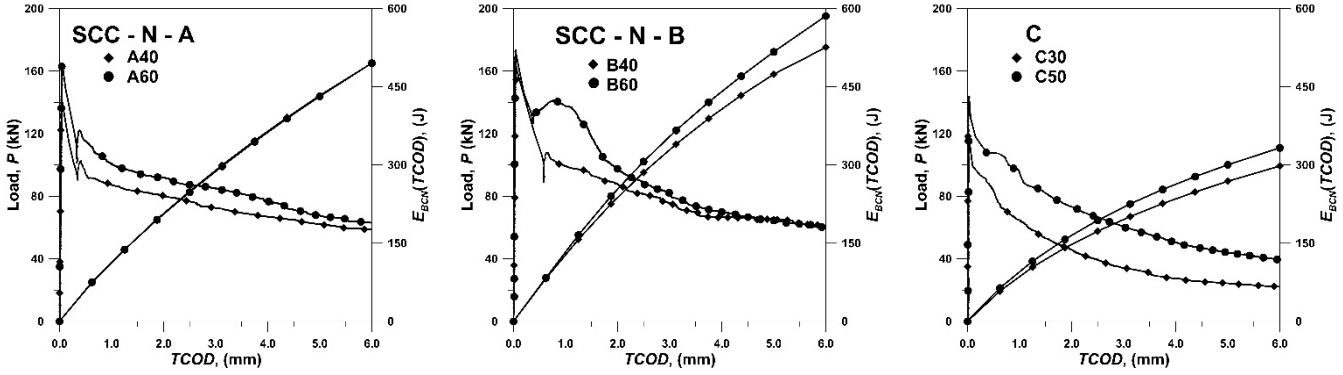

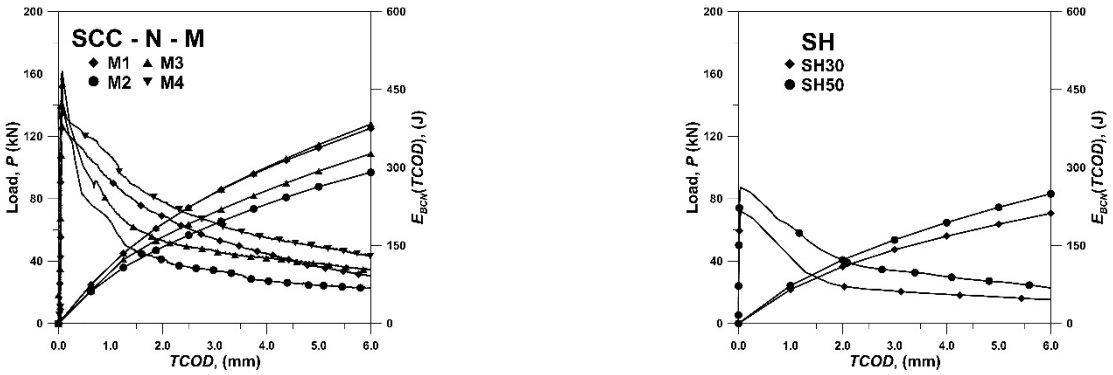

Figure 5. Typical $P - TCOD$ curves obtained with BCN tests, and average curves $E_{BCN} - TCOD$.

7. CORRELATIONS BETWEEN THE 3PB AND BCN TESTS

From the results of the tests already presented, analyses were performed to establish the correlations between T_{EN} and E_{BCN} and between the residual strengths $F_{R,j}$ and $f_{ct,Rx}$, obtained through both tests.

7.1. Correlation between T_{EN} and E_{BCN}

Equivalent values of the toughness T_{EN} and the dissipated energy E_{BCN} corresponding to the same mean crack opening w are presented in Tables 5 and 7 and in Figure 6. In these diagrams it is possible to estimate the T_{EN} with an expression of the following type:

$$T_{EN}\left(E_{BCN}\ (TCOD, V_f)\right) = a\left[E_{BCN}(TCOD, V_f)\right]^b \quad (8a)$$

where a and b are two experimental parameters which depend on the characteristics of each FRC. Table 9 presents the values of a and b obtained from the nonlinear regressions performed with the results of each studied FRC. These two parameters depend on the type of concrete, i.e., either conventional (C), self-compacting (SSC) or shotcrete (SH). In conventional concrete the value of a decreases when the amount of fibers increase, while in all fluid concretes (SCC and SH) the value of a increases (Table 9). On the other hand,

the behavior of parameter b is the opposite. In conventional concrete this parameter increases for higher amount of fibers, while decreases in fluid concretes.

When analyzing the effect of the aspect ratio of the fiber on the parameters, a and b, in fluid concretes, the increment of the aspect ratio produces the increment of a parameter. This confirms that through the 3PB test it is possible to better notice the increment of the fiber efficiency, when the aspect ratio increases. On the other hand, b parameter decreases when the fibers' aspect ratio increases, producing a more linear relation between T_{EN} and E_{BCN}.

When comparing self-compacting concretes of normal strength, SCC-N, with those of high strength, SCC-H, it can be observed that in both concretes, a parameter almost doubles when the fiber contents grow from 40 to 60 kg/m^3 but b parameter is almost constant for the fiber contents analyzed. According to the latter, it appears clear the existence of preferential orientation of fibers in the longitudinal direction of the beam specimen. This direction is the one with largest tension stresses during the tests and normally fibers oriented in the longitudinal direction bridge the cracks in a very good almost perpendicular direction. Then, beam test could overestimate the efficiency of fibers due to this preferential orientation along the beam axis. On the other hand, since BCN test uses a smaller and cylindrical specimen, it does not allow for noticeable preferential fiber orientation. Fibers are randomly oriented and, in addition, during the test tension forces are perpendicular to radial planes. Then, the beneficial effect of a larger fiber content on the toughness is not so noticeable.

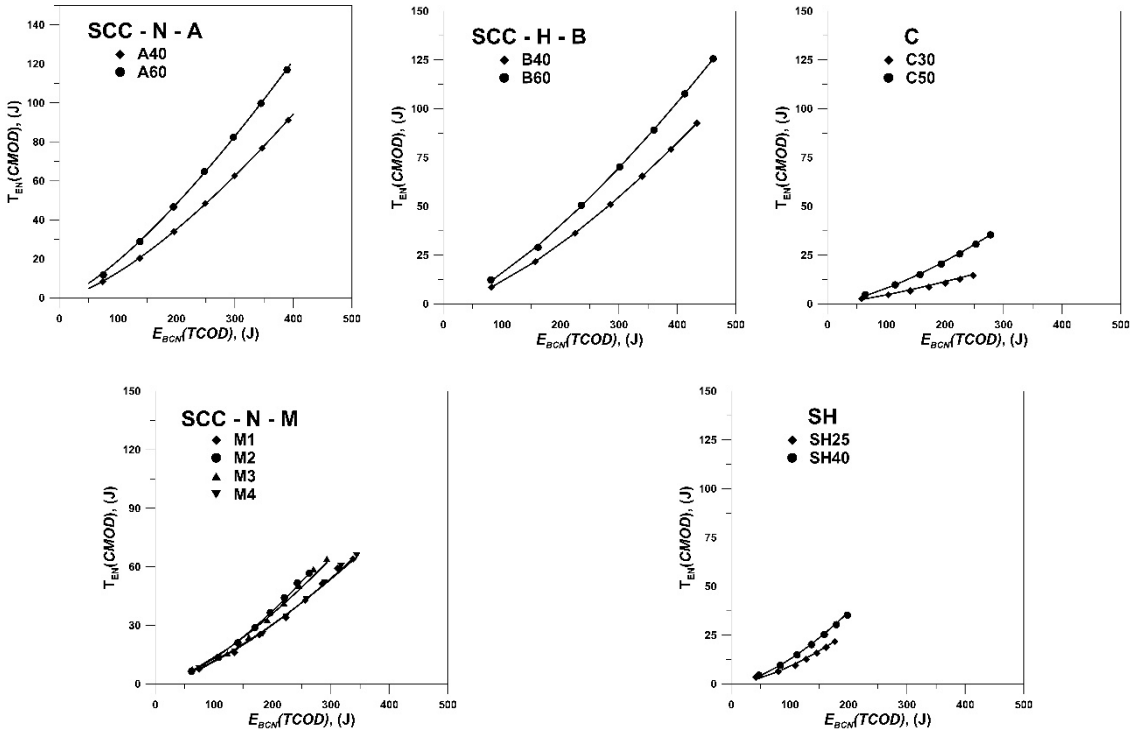

Figure 6. Experimental relationships between T_{EN} and E_{BCN} of each concrete studied, along with their respective exponential trend line (Eq. 8a).

1

2 Table 9. Parameters of correlations between T_{EN} and E_{BCN} of each FRC studied.

Concrete		f_c (MPa)	Fiber content (kg/m^3)	V_f (%)	λ_f l_f/d_f	a	b	r^2
Type	Ref.							
C	C30	45	30	0.38	47.6	0.012	1.290	0.995
	C50	44	50	0.64		0.009	1.465	0.999
SCC – N	A40	46	40	0.51	84.5	0.019	1.424	0.999
	A60	50	60	0.77		0.040	1.339	0.999
	M1	49	30	0.38	63.6	0.009	1.519	0.999
	M2	45			64.5	0.007	1.623	0.999
	M3	52			66.7	0.006	1.649	0.998
	M4	49			71.2	0.010	1.514	0.999

SCC – H	B40	76	40	0.51	84.5	0.016	1.430	1.000
	B60	79	60	0.77		0.028	1.370	1.000
SH	SH25	41	25	0.32	63.6	0.007	1.556	0.994
	SH40	45	40	0.51		0.013	1.498	0.999

Using the relationships between parameter a and b with volume substitution, V_f, a non-linear regression was established obtaining the expression:

$$T_{EN}\left(E_{BCN}(TCOD), V_f\right) = \frac{0.075\, V_f^{2.278}}{\alpha}\left[E_{BCN}\left(TCOD, V_f\right)\right]^{\frac{1.263\, V_f^{-0.224}}{\beta}} \quad (8b)$$

where α and β are empirical parameters which depends on the concrete type, adopting the values given in Table 10.

Table 10. Expressions to obtain the experimental parameters of the correlations: α and β for toughness correlation and γ and δ for residual strength correlation.

Parameter	Concrete			
	C	SCC–N	SCC–H	SH
α	$8.775\, V_f - 2.63$	1.0	$1.95\, V_f$	$2.60\, V_f - 0.03$
β	$-0.975 V_f + 1.58$	1.0	$-0.195\, V_f + 1.15$	$-0.52\, V_f + 1.22$
γ	$-3.9\, V_f + 5.0$	1.0	$1.17\, V_f + 0.5$	$0.52\, V_f + 1.33$
δ	$-1.755\, V_f + 1.78$	1.0	$-0.975\, V_f + 1.5$	$-1.5\, V_f + 1.62$

With the $E_{BCN}(TCOD, V_f)$ values given in Table 7 and using equation (8b), the values of $T_{EN}(E_{BCN}(TCOD), V_f)$ were estimated, leading to the results shown in Figure 7a. Most of the results obtained with the correlations fit the experimental results satisfactorily, been the A40, M2, and M3 concretes the ones which present the largest differences. Complementarily, Figure 7b exhibit the differences between the estimated

$T_{EN}(E_{BCN}(TCOD), V_f)$) values and the experimental $T_{EN}(CMOD)$ values (Table5), where it can be observed that in most of the FRC studied, the greatest differences are found for $CMOD$ = 1.0 mm ($TCOD$ = 1.250 mm). For larger crack opening values, the differences are less than ±10%, except for the A40, M1 and M4 concretes, where the differences reach a maximum of 19%.

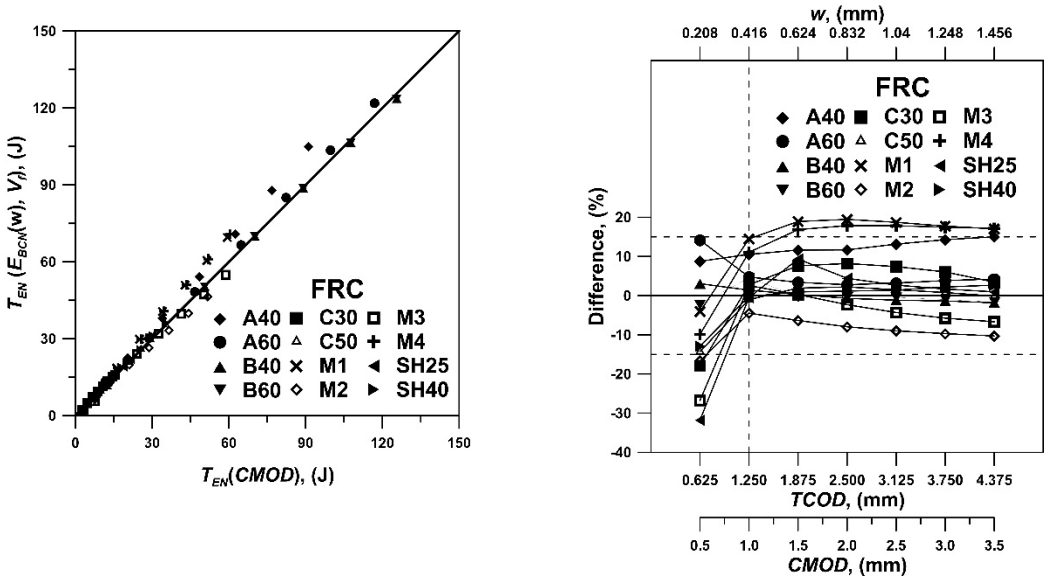

(a) **(b)**

Figure 7. (a) Deviation of estimated values of $T_{EN}(E_{BCN}(TCOD), V_f)$, with respect to the experimental values $T_{EN}(CMOD)$; (b) Percentage difference between the experimental values $T_{EN}(CMOD)$ and the values of $T_{EN}(E_{BCN}(TCOD), V_{f)})$.

7.2. CORRELATION BETWEEN $F_{R,j}$ AND $f_{ct,Rx}$

Considering that design requirements in the projects normally refer to the residual strength values defined in the standard EN – 14651, computed with equation (1), this section establishes an equivalence between the residual strengths $F_{R,j}$ and $f_{ct,Rx}$. This equivalence is intended in a way that both characterization and aptitude tests can be done using the parameters established from the bending test and, later, the systematic quality control during the works can be performed through the Barcelona Test.

In contrast to the trends observed with the relationship between $E_{BCN}(TCOD)$ and $T_{EN}(CMOD)$, there is no unique trend for the relation between the residual strengths obtained in the bending tests, $F_{R,j}$, with those reached in the BCN tests, $f_{ct,Rx}$. However, by establishing the ratio $F_{R,j}/f_{ct,Rx}$, the trends presented in Figure 9 fit the form:

$$\frac{F_{R,j}}{f_{ct,Rx}} = c\,TCOD^{d} \tag{9a}$$

where c and d are also experimental parameters which depend on the concrete type and the fiber content of FRC, as can be seen Table 11, where the values of these parameters are given for each studied concrete. From this table, it can be observed that the parameter c increases when fiber amount increases. With respect to d-parameter, this exhibits the same trend for conventional concrete, while shows the opposite trend for all the fluid concretes.

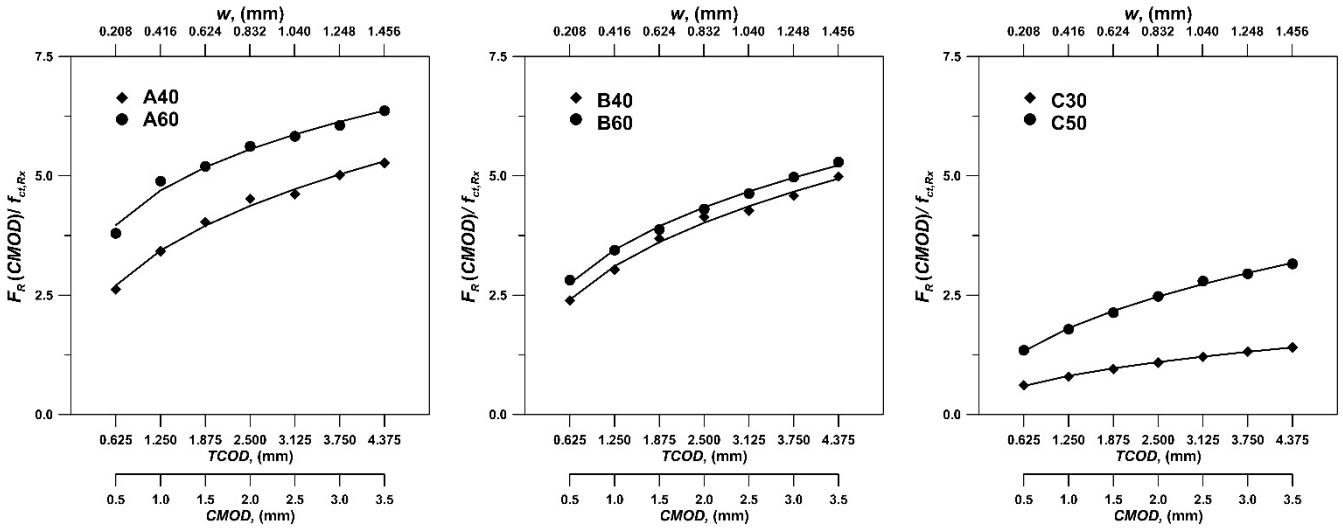

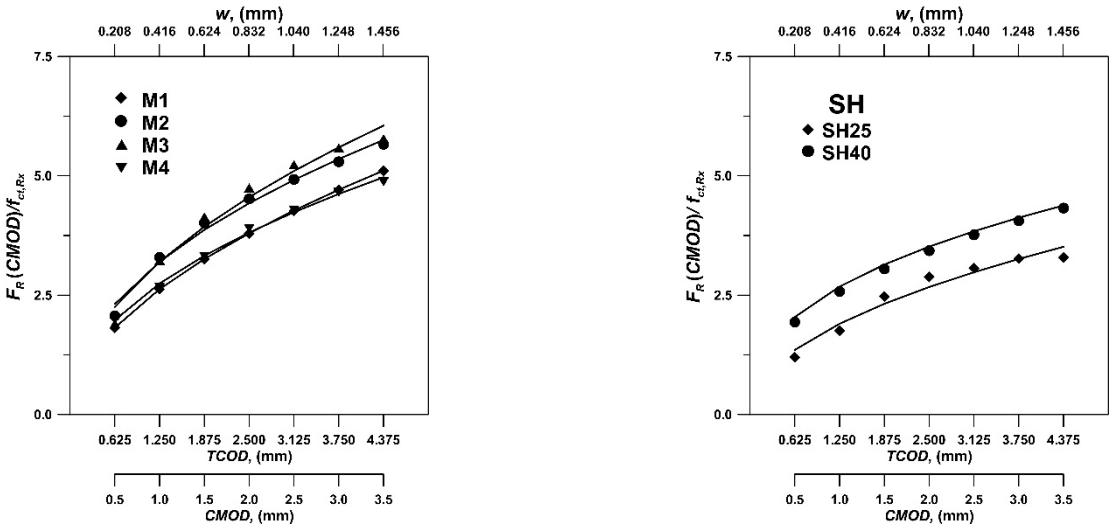

Figura 8. Experimental relationships $f_{R,j}/f_{ct,Rx} - CMOD$ of each concrete, along with their respective trend line.

1

2 Table 11 – Parameters of the nonlinear correlations for $F_{R,J}/f_{ct,Rx}$ ratio obtained with

3 each FRC.

Concrete		f_c (MPa)	V_f (%)	c	d	r^2
Type	Reference					
C	C30	45	0.38	0.735	0.439	0.999
	C50	44	0.64	1.638	0.449	0.997
SCC – N	A40	46	0.51	3.182	0.347	0.991
	A60	50	0.77	4.446	0.243	0.983
	M1	49	0.38	2.334	0.531	0.994
	M2	45		2.883	0.468	0.988
	M3	52		2.861	0.508	0.976
	M4	49		2.471	0.474	0.996

SCC – H	B40	76	0.51	2.862	0.370	0.991
	B60	79	0.77	3.206	0.330	0.996
SH	SH25	41	0.32	1.705	0.490	0.957
	SH40	45	0.51	2.456	0.392	0.980

Through a non-linear regression, an explicit expression allows to correlate directly both residual strengths, $F_{R,j}$ from $f_{ct,Rx}$ was obtained, which depends on the concrete type and the fiber reinforcement content:

$$F_{R,j}\left(f_{ct,Rx}(TCOD), V_f\right) = \left[\frac{5{,}448 \cdot V_f^{0.746}}{\gamma} TCOD^{\frac{0.182 V_f^{-1.058}}{\delta}}\right] \times f_{ct,Rx}(TCOD) \qquad (9b)$$

where γ and δ are empirical parameters which depends on the concrete type, adopting the values given in Table 10.

The accuracy of this correlation is demonstrated comparing the computed $f_{R,j}(f_{ct,Rx}(TCOD), V_f)$, using the Barcelona test residual strengths presented in Table 8, with the experimental ones $f_{R,j}(CMOD)$. Figure 9a shows this comparison which is significantly accurate. The largest deviations between the experimental and correlated values are in the M and SH25 concrete series. Figure 9b presents the differences between the estimated values $f_{R,j}(f_{ct,Rx}(TCOD), V_f)$ and the experimental ones $f_{R,w}$, showing that the differences are less than ±15% for most of the studied concretes and, in the case of C30, C50, A60, B40, B60 and SH40 series are less than 7%. This demonstrates the good fitting of this new correlations developed using the experimental values, which allow to estimate the residual strength with differences smaller than the coefficient of variation of the original experimental results.

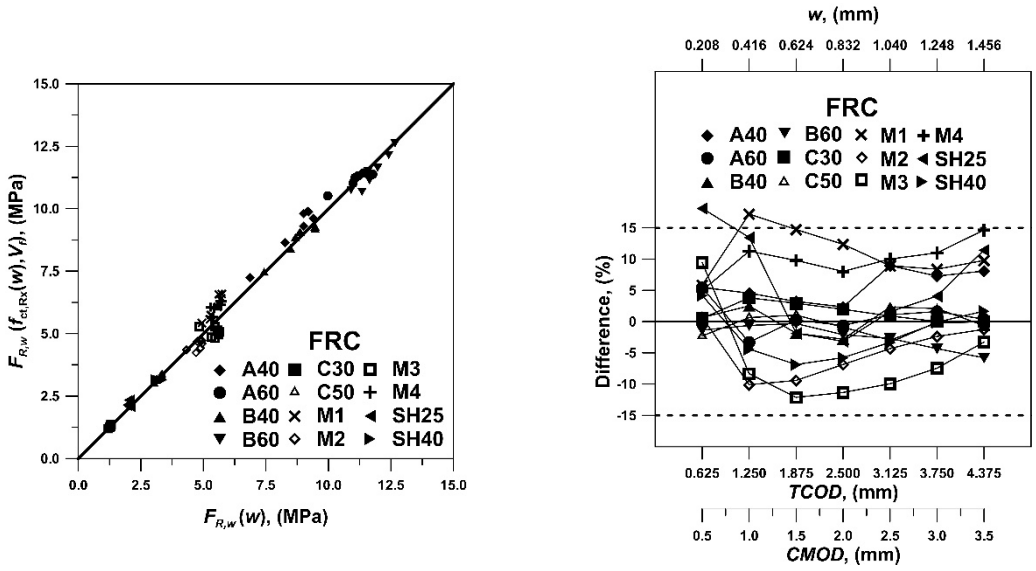

(a) **(b)**

Figure 9. (a) Deviation of estimated values $f_{R,j}(f_{ct,Rx}(TCOD),V_f)$, with respect to the experimental ones $f_{R,j}(CMOD)$; (b) Percentage difference between the experimental and the estimated values.

8. VALIDATION OF THE CORRELATIONS

The results of an additional experimental campaign allowed to validate the correlations. That campaign included 10 beams and 8 cylinder specimens of SCC – N (cement type IP: 380 kg/m^3; water: 150 kg/m^3; sand: 1060 kg/m^3; gravel: 880 kg/m^3; water reducer admixture: 0.83 kg/m^3; plasticizer admixture: 1.93 kg/m^3; f_c = 34.8 MPa) reinforced with 40 kg/m^3 of steel fibers type Dramix 4D 65/60-BG© (l_f = 60 mm; d_f = 0.9 mm; λ_f = 65; f_{st} = 1600 MPa; N° fibers/kg: 3149), which were subjected to double punching and to bending tests, respectively. Both, the toughness and the residual strengths were determined.

The FRC was cast in a vertical axis paddle mixer and the 10 beams and the 8 cylinders were molded. The specimens were demolded after 24 hr and kept in a fog-room until tests. The tests were performed at age of 28 days, according to the standards EN - 14651

and UNE 83 515, obtaining the results given in Table 12 and 13, and the average curves are plotted in Figure 10.

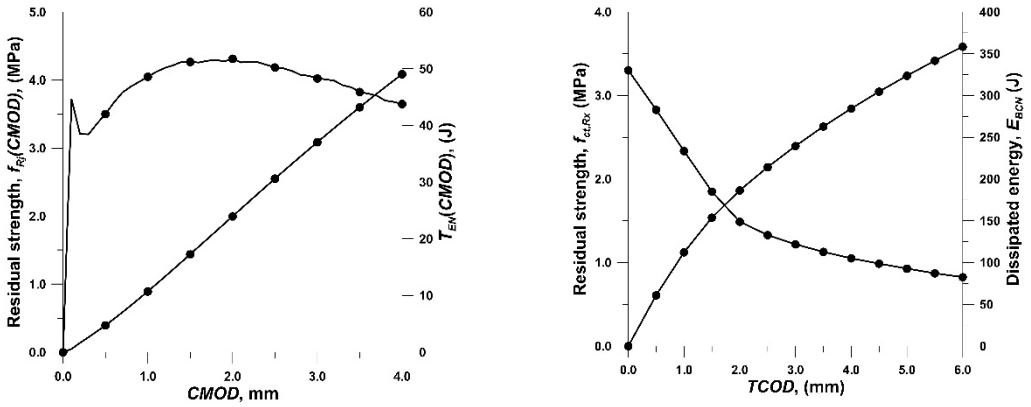

(a) (b)

Figure 10. Validation tests results: (a) average bending tests EN – 14651; (b) average double punching tests UNE 83 515.

Replacing the values of V_f= 0.513 and the mean dissipated energy, $E_{BCN}(TCOD)$ and residual strengths $f_{ct,Rx}(TCOD)$ obtained with BCN tests in the equations (8b) and (9b), flexural toughness, $T_{EN}(E_{BCN}(TCOD), V_{f)})$, and residual strength, $f_{R,j}(f_{ct,Rx}(TCOD), V_f)$, were estimated, reaching the values also presented in Tables 12 y 13, respectively, along with their CoV in brackets.

Table 12. Validation of Eq. (8b).

$TCOD$ (mm)	$E_{BCN}(TCOD)$ (J)	$CMOD$ (mm)	$T_{EN}(CMOD)$ (J)	$T_{EN}(E_{BCN}(TCOD), V_{f)})$ (J)	Diff. (%)
0.625	55.1 (6.8)	0.5	5.9 (27.8)	5.9	-0.87
1.25	101.1 (7.0)	1.0	13.5 (5.1)	14.3	5.96
1.875	147.2 (9.5)	1.5	21.9 (16.4)	24.8	13.41

2.500	192.8 (8.2)	2.0	30.5 (24.8)	36.9	20.74
3.125	221.0 (8.7)	2.5	39.0 (29.9)	45.1	15.43
3.75	246.4 (9.1)	3.0	47.0 (33.9)	52.8	12.31
4.375	269.8 (9.5)	3.5	54.8 (36.4)	60.3	10.19

Table 13. Validation of Eq. (9b).

$TCOD$ (mm)	$f_{ct,Rx}(TCOD)$ (MPa)	$CMOD$ (mm)	$f_{R,j}(CMOD)$ (MPa)	$f_{R,j}(f_{ct,Rx}(TCOD), V_f)$ (MPa)	Diff. (%)
0.625	2.827 (7.0)	0.5	3.502 (15.7)	4.857	38.69
1.25	2.336 (7.6)	1.0	4.050 (18.2)	4.527	11.78
1.875	1.785 (12.6)	1.5	4.267 (20.0)	4.099	-3.93
2.500	1.330 (16.7)	2.0	4.315 (20.2)	3.678	-14.77
3.125	1.194 (16.9)	2.5	4.187 (20.5)	3.534	-15.58
3.75	1.091 (16.2)	3.0	4.026 (21.2)	3.419	-15.07
4.375	1.002 (17.9)	3.5	3.826 (20.7)	3.313	-13.40

These results in Tables 12 and 13 show that the equations 8b and 9b allow to determine the properties of the FRC with differences smaller than the average values of the CoV of the bending test results.

According to the results, it is worth noting that the V_f and the concrete type parameters are more significant than fiber type or compressive strength of concrete for the proposed correlations.

Although a simple general expression would facilitate the application of the BCN test for the control of the FRC, this is not evident because there are many factors that can influence, from the features and strength of the concrete to the type of fiber used.

However, from the proposed correlations and with a greater number of results it is possible that a more general correlation could be found.

9. SCATTER OF RESULTS

From the point of view of quality control of FRC properties, the normal high scatter of the experimental results for the toughness and the residual strength obtained by means of 3PB produces characteristic values significantly lower compared to the average ones. Results in Tables 5 and 6 show average values of CoV of 17.9% and 19.8% for toughness and residual strengths, respectively. Cavalaro and Aguado (2015) reported that the CoV is in the average above 15% for the residual strengths of concretes reinforced with 40 kg/m^3 or less of steel fibers, which leads to characteristic values far below the average measured residual strength. Nevertheless, several authors indicate that the real scatter on the post–cracking behavior of FRC reduces considerably with the increase of the cracking surface, which is evident when real–scale elements are tested, where a CoV of 6.8% on the average was reached by De La Fuente *et al*., 2012. Such trend shows a possible contradiction in the design based on characteristics values determined from small – scale tests which might not be representative of large – scale structures.

Cavalaro and Aguado (2015) proposed a new expression to determine the CoV, which take in account the structure size, obtaining values of CoV for large-scale structures around 50% lower than the value of CoV reached for small-scale structure.

From CoV reached with results of BCN tests, showed in Tables 7 and 8, can be obtained averages values of 10.1% and 13.7% for dissipated energy and residual strengths respectively. These CoV are 56% and 69% lower than values reached with bending tests, then might meaning that CoV of BCN tests results are closer to CoV of large – scale structures and, then, can help to better determine the characteristic values of real – scale structures.

10. CONCLUSIONS

An equivalence between the 3PB test and the BCN test was established using geometrical relations based on the mean crack width, *w*, resulting in $TCOD = 1.25\ CMOD$.

The absolute errors in the flexural toughness based on the BCN test dissipated energy were lower than 15% for most of the FRC specimens studied, for *TCOD* values greater than 1.25 mm, or equivalently, for *CMOD* values greater than 1.00 mm.

Similarly, correlations were obtained that allow continuously obtaining the equivalence between the residual strengths measured with the 3PB test and the cylinder subjected to the BCN test. For fiber contents between 25 and 60 kg/m^3, the absolute value of the relative differences when estimating the residual strengths with the proposed expressions were less than 18%.

The results show that all correlations between both tests strongly depend on the type of concrete tested, be it conventional or self-compacting, and on the fiber content, which was quantified throughout the investigation by means of volumetric substitution.

The proposed expressions establish continuous equivalences between the flexural test and the BCN test, which favors the use of the BCN test for the systematic control of construction projects, particularly for fiber-reinforced shotcrete in underground construction.

The differences obtained by estimating the toughness and residual strengths values in the flexural test from the BCN test results are lower than the variation coefficients of the experimental results used in the investigation, which demonstrates the good fitting of the proposed expressions.

11. ACKNOWLEGEMENTS

This research was supported by Fondecyt Project “Use of the Generalized Barcelona Test for Characterization and Quality Control Of Fiber Reinforced Shotcretes In Underground

Mining Works", N°1150881. Third author thanks to Ministerio de Economía Industria y Competitividad of Spain the support of Proyect BIA2016-78742-C2-1-R Seguridad en aplicaciones estructurales de hormigón reforzado con fibras.

REFERENCES

CEB-FIP, "Model Code – First Complete Draft," *FIB Bull vol*. 1, V. 55, 2010, pp. 1–318.

ACI, "Building Code Requirements for Structural Concrete (ACI 318M1-14) and Commentary (ACI 318RM-14)," ACI Committee 318, Jan. 2017, 524 pp.

EFNARC, "European Specification for Sprayed Concrete," 1996, 30 pp.

EN 14487-1-2005 sprayed concrete - part 1: definitions, specifications and conformity.

ACI, "Report on Measuring Mechanical Properties of Hardened Fiber–Reinforced Concrete 544.9R-17," Report of Committee 544, Michigan, 2017, 52 pp.

RILEM TC 162, "TDF Test and Design Methods for Steel Fibre Reinforced Concrete: Bending Test," *Materials and Structures*, V. 35, 2002, pp. 579–582.

Barragán, B., Gettu, R., Martín, M. A., Zerbino, R. L., "Uniaxial Tension Test for Steel Fibre Reinforced Concrete – A Parametric Study," *Cement and Concrete Composites.* V. 25, No. 7, Oct., 2003, pp. 767–777.

Chao, S. H., Karki, N. B., Cho, J. S., Waweru, R. N., "Use of Double Punch Test to Evaluate the Mechanical Performance of Fiber Reinforced Concrete," In Parra-Montesino, Reinhardt, Naaman, editors. Proceedings of the 6th International Workshop on High Performance Fiber Reinforced Concrete Composites (HPFRCC 6), Ann Arbor, Michigan, 2012, pp.27–34.

Carmona, S., Aguado, A., Molins, C., "Generalization of the Barcelona Test for the Toughness Control of FRC," *Materials and Structures*, V. 45, Nº 7, July. 2012, pp. 1053–1069.

Cavalaro, S., and Aguado, A., "Intrinsic Scatter of FRC: An Alternative Philosophy to Estimate Characteristic Values," *Materials and Structures*, V. 48, No. 11, Nov. 2015, pp.

3537–3555.

Molins C., Aguado A. and Saludes S., “Double Punch Test to Control the Energy Dissipation in Tension of FRC (Barcelona Test),” *Material and Structures*, V. 42, 2009, pp. 415–425.

AENOR, “UNE 83-515. Hormigones con fibras. Determinación de la resistencia a fisuración, tenacidad y resistencia residual a tracción. Método Barcelona,”. AEN/CTN 83–Hormigón, Madrid, 2010, pp. 8 (in Spanish).

Carmona, S., Aguado, A., Molins, C., “Characterization of the Properties of Steel Fiber Reinforced Concrete by Means of the Generalized Barcelona Test,” *Construction and Building Materials*, V. 48, 2013, pp. 592–600.

Aire, C., Carmona, S., Aguado., Molins, C., “Double-Punch Test of Fiber-Reinforced Concrete: Effect of Specimen Origin and Size,” *ACI Materials Journal*, V. 112, No 2. 2015, pp 199–208.

Pros, A., Diez, P., Molins, C., “Numerical Modeling of the Double Punch Test for Plain Concrete,” *International Journal of Solids and Structures*, V. 48, 2011, pp. 1229–1238.

Pros, A., Diez, P., Molins, C., “Modeling Steel Fiber Reinforced Concrete: Numerical Immersed Boundary Approach and a Phenomenological Mesomodel for Concrete–Fiber Interaction,” *International Journal for Numerical Methods in Engineering*, V. 90, 2012, pp. 65–86.

Pujadas, P., Blanco, A., Cavalaro, S., De la Fuente, A., Aguado, A., “Analytical Model that Allows a Generalization of the Barcelona Test by Using the Axial Displacement to Determine the Toughness of the FRC,” *Journal of Civil Engineering and Management*, V.19, No. 2, 2013, pp. 259–271.

Kim, J., Lee, G. P., Moon, D. Y., “Evaluation of Mechanical Properties of Steel-Fibre-Reinforced Concrete Exposed to High Temperatures by Double-Punch Test,” *Construction and Building Materials*, V. 79, 2015, pp. 182–191.

Carmona, S., Molins, C., Aguado, A., Mora, F., “Distribution of Fibers in SFRC Segments for Tunnel Linings,” *Tunnelling and Underground Space Technology*, V. 51, Jan. 2016, pp 238–249.

Geocontrol Andina, “Especificaciones Técnicas Detalladas; Trabajos en mina, Línea 2 y Ramal Av. Faucett–Av. Gambetta de la Red Básica del Metro de Lima y Callao,” Perú, 2015, 78 pp.

Carmona, S., “Informe Técnico Capacidad de Absorción de Energía de Shotcrete Reforzados con Fibras Mediante el Ensayo Barcelona”, ” Internal Report, Valparaíso, Chile, 2017, pp. 15 (in Spanish).

CEN, “EN 14651: Test Method for Metallic Fibered Concrete–Measuring the Flexural Tensile Strength (Limit of Proportionality (LOP), Residual),” European Committee for Standardization, Brussels, 2005.

ACI, “Report on Indirect Method to Obtain Stress-Strain Response of Fiber–Reinforced Concrete (FRC) ACI 544.8R-16,” ACI Committee 544, Michigan, 2016, 28 pp.

Molins, C., Aguado, A. and Guàrdia, J. (2008), “Control de la resistencia a fisuración y tracción residual de HRFA mediante el ensayo Barcelona”, IV Congreso Internacional de Estructuras de la Asociación Científico-técnica del Hormigón Estructural, held in Valencia (Spain), pp 263-264.

Monsó, A., “Análisis del comportamiento del hormigón reforzado con fibras para el ensayo Barcelona y de flexotracción,” Departamento de Ingeniería de la Construcción, Universidad Politécnica de Cataluña, Barcelona, Spain, 2011, pp. 208 (in Spanish).

Carmona, S., “Resultados de Ensayos de Hormigones Reforzados con Fibras – Proyecto Fondecyt No 1150881” Internal Report, Valparaíso, Chile, 2017, pp. 105 (in Spanish).

Laranjeira, F., Grünewald, S., Walraven, J., Blom C., Molins, C., Aguado, A., “Characterization of the orientation profile of steel fiber reinforced concrete”, *Materials and Structures*, V. 44, No. 6, July. 2011, pp. 1093–1111.

Blanco, A., Pujadas, P., De la Fuente, A., Cavalaro, S., Aguado, A., “Influence of the Type of Fiber on the Structural Response and Design of FRC Slabs”, *Journal of Structural Engineering*, V. 142, No. 9, Sept. 2016.

De la Fuente, A., Escariz, R.C., Figueiredo, A.D., Molins, C., Aguado, A., “A new design method for Steel fiber reinforced concrete pipes”. *Construction and Building Materials*, Vol. 30, 2012, pp. 546 – 555.